E-cigarette constituents propylene glycol and vegetable glycerine decrease glucose uptake and its metabolism in airway epithelial cells *in vitro*.

Woodall M, Jacob J, Kalsi K, [1]Schroeder V,[2]Davis E, [2]Kenyon, B, [1]Garnett JP, [2]Tarran R & Baines DL.

Institute for Infection and Immunity, St George's, University of London, Tooting, London SW17 0RE. [1] Immunology & Respiratory Diseases Research, Boehringer Ingelheim Pharma GmbH & Co. KG, Birkendorfer Str. 65, 88397 Biberach an der Riß, Germany, [2] Marsico lung Institute & Dept Cell Biology and Physiology, University of North Carolina at Chapel Hill, Chapel Hill, NC, USA.

Running Title: PG/VG decreases glucose uptake and metabolism

Abstract

Electronic nicotine delivery systems, or e.cigarettes utilise a liquid solution that normally contains propylene glycol (PG) and vegetable glycerine (VG) to generate vapour and act as a carrier for nicotine and flavourings. Evidence indicated these 'carriers' reduced growth and survival of epithelial cells including those of the airway. We hypothesised that 3% PG or PG mixed with VG (3% PG:VG, 55:45) inhibited glucose uptake in human airway epithelial cells as a first step to reducing airway cell survival.

Exposure of H441 or human bronchiolar epithelial cells (HBEC) to PG and PG/VG (30-60 minutes) inhibited glucose uptake and mitochondrial ATP synthesis. PG/VG inhibited glycolysis. PG/VG and mannitol reduced cell volume and height of air-liquid interface cultures. Mannitol but not PG/VG increased phosphorylation of p38 MAPK. PG/VG reduced TEER which was associated with increased transepithelial solute permeability. PG/VG decreased FRAP of GFP linked glucose transporters GLUT1 and GLUT10 indicating that glucose transport function was compromised. Puffing PG/VG vapour onto the apical surface of primary HBEC for 10 mins to mimic the effect of e.cigarette smoking also reduced glucose transport.

In conclusion, short term exposure to PG/VG, key components of e.cigarettes, decreased glucose transport and metabolism in airway cells. We propose that this was a result of PG/VG reduced cell volume and membrane fluidity, with further consequences on epithelial barrier function. Taken together, we suggest these factors contribute to reduced defensive properties

of the epithelium. We propose that repeated/chronic exposure to these agents are likely to contribute to airway damage in e-cigarette users.

.

Introduction

Electronic nicotine delivery systems (ENDS), more commonly known as e.cigarettes, are used to deliver nicotine as an alternative to the use of tobacco.
. These devices utilise a liquid solution which is drawn over a heating element to produce a vapour which is then inhaled giving rise to the term 'vaping'. The solutions normally contain the humectants propylene glycol (propane-1,2-diol; PG) and vegetable glycerine (propane-1,2,3-triol; VG) to generate the vapour and act as carriers for nicotine and flavourings. The viscosity of VG is refractory to its sole use in electronic cigarettes. PG and VG are therefore mixed in a wide range of ratios by suppliers of vape products and by end users. Increased PG provides a 'throat hit' more like that of cigarette smoking and is thought by some users to improve the carriage of flavourings (20, 43).

There is much debate around the safety of e-cigarettes and the effect of repeated inhalation of these products on the airway. Evidence has indicated the carriers alone may have cytotoxic effects. Both PG and VG are widely used in the food and cosmetics industry. However, the use of PG as a solvent for drugs delivered intravenously was noted to cause side effects in patients including lactic acidosis and renal insufficiency (4, 53). Exposure to PG vapour was found to cause upper airway irritation (50) and following a systematic review of the health effects of e-cigarettes, concern remained regarding the effect of PG on the airway (38). *In vitro*, PG (at concentrations estimated to be found in the plasma of patients receiving intravenous medication) was shown to have acute cytotoxic and metabolic effects on renal

proximal tubule cells (30-33). Furthermore, exposure to PG/VG at a ratio often used in vapes, was found to reduce growth and survival of human embryonic kidney cells and Calu-3 airway epithelial cells (31, 41, 42).

The mechanisms underlying the effects of PG/VG on cell proliferation and viability, particularly in the airway are unclear. As glucose uptake is a key metabolic requirement for cell growth, survival and is critical for the normal function of the airway epithelium, we hypothesised that exposure to PG or PG mixed with VG (PG/VG) at a ratio frequently used in vapes would reduce glucose uptake human airway epithelial cells as a first step to altered cell metabolism.

We therefore investigated the effects of PG and PG/VG (55:45) on glucose uptake in proliferating human H441 and primary bronchial airway epithelial (HBE) cells in submerged culture and when cultured at air-liquid interface (ALI) to more closely represent the *in vivo* airway. We exposed cells to PG or PG/VG applied to the culture medium and vaporised to the apical (luminal) surface of (ALI) cultures. We also explored potential mechanisms determining the action of PG/VG on glucose uptake and metabolism including, osmotic effects and the stability of key glucose transporters known to be expressed in the membrane domain of airway cells using fluorescence recovery after photobleaching (FRAP).

Materials and Methods

Epithelial cell culture

Human H441 airway epithelial cells (from ATCC, Manassas, VA, USA) were cultured in RPMI-1640 media containing 10% foetal calf serum (FCS) (Invitrogen, UK), 10 mM glucose,

2 mM glutamate, 1 mM sodium pyruvate, 10 µg/mL insulin, 5 µg/mL transferrin, 7 ng/mL sodium selenite, 100 U/mL penicillin and 100 µg/mL streptomycin. HBEC transduced with human polycomb complex protein, *BMI-1 (HBEC-BMI-1)* were obtained from Prof S Hart, ICH, UCL and were cultured as previously described (35). Primary human bronchial epithelial cultures (HBECs) were obtained by the UNC CF Center Tissue Core under protocols approved by the UNC Institutional Committee for the Protection of the Rights of Human Subjects as described. H441, BMI1-transduced HBEC and primary cells were transferred onto clear Transwell® (Costar) inserts (1.12 cm^2 area, 0.45-µm pore size) and grown at air-liquid-interface (ALI) to form confluent fully differentiated monolayers as described (39, 45, 46). H441 cells were studied 10-14 days post seeding, HBEC were studied 3-5 weeks post-seeding. Transepithelial electrical resistance (TEER) was measured using an electrovoltometer (EVOM) with chopstick electrodes (WPI, UK) and corrected for resistance associated with the Transwell supports. Human embryonic kidney (HEK293) cells were grown in DMEM + 10% FCS as previously described (42).

PG (3%) or PG/VG (55:45, 3%) was applied to the medium (or directly to the apical (luminal) surface for time periods of 0-24 hours, or the cells were exposed to E-cigarette vapour E-cigarette aerosols were generated using a Sigelei FuChai 200W-TC device with a Crown stainless steel subtank with a 0.25 Ω SUS316 dual coil from Uwell as previously described in detail (15) . We typically generated 70 mL puffs drawn over approximately 5 seconds and dispensed at 0.84 L/min at 100 W. This meant that 20 puffs from our vaping system delivered a concentration equivalent to ~0.38% e-liquid (vol/vvol) per well in 100 µl of PBS or mediaMannitol (7.4% w/v was used as an osmotic control in some experiments which gave a similar osmoliarity to that of 3% PG/VG at 408.5 mOsm). All solutions were purchased from Sigma-Aldrich, UK.

Measurement of cell shrinkage.

For HEK293T cells, cells were cultured on glass coverslips for 24 h. Epifluorescence measurements were performed using a Nikon Ti-S microscope with Hamamatsu Flash 4.0 Camera and Ludl Filter wheels and a 20 x dry plan fluor lens. HBECs were bilaterally loaded with 3 mM calcein-AM (Invitrogen, USA) for 30 min at 37°C. (12) Calcein-loaded HBECs were observed by XZ confocal microscopy. Shrinkage was initiated with the mucosal addition of 200 μL of solution (3% PG/VG or mannitol) and cell height and serosal bath intensity were tracked over time (47).

HBEC height and confocal airway surface liquid (ASL) height measurements.

To measure the height of the ASL, PBS (20 μl) containing 2 mg/ml rhodamine-dextran (10 kDa; Invitrogen, USA) was added to cultures at the start of the experiment and all possible fluid was aspirated with a Pasteur pipette to bring ASL volume down to minimal levels.15 predetermined points were automatically XZ scanned using a confocal microscope (Leica SP8; glycerol 63 X immersion lens) as described (9). Cultures were returned to the incubator between time points. For all studies, perfluorocarbon (PFC) was added mucosally during imaging to prevent evaporation of the ASL.

Permeability assay

Culture medium was replaced with Hanks Balanced Salt Solution (HBSS) (Sigma-Aldrich, UK) and cells were incubated with either HBSS alone or with 3% PG/VG in the apical solution. After 30 minutes, the apical solution was replaced with 0.5 mL HBSS with 10 μM Na-fluorescein (MW = 367 Da, Sigma-Aldrich). Samples of 0.1mL were removed from the basolateral bath at 0, 30, 60 and 90 minutes and fluorescence was measured in black, 96-well

plates using a GloMax fluorescence plate reader with excitation and emission wavelengths of 460 nm and 515 nm respectively.

Glucose uptake

Glucose uptake across the cell membrane was measured using either ^{14}C-D-glucose as previously described (23) or using the Uptake Glo luminescent assay (Promega, UK). In brief, cultured cells were washed twice with glucose-free transport medium (15 mM HEPES buffer (pH 7.6), 135 mM NaCl, 5 mM KCl, 1.8 mM $CaCl_2$ and 0.8 mM $MgCl_2$), then incubated for 15 min to deplete intracellular glucose. Uptake was initiated by replacing with 0.5 ml transport medium containing 1.0 μCi ^{14}C- D-glucose + 10 mM of non-radiolabelled D-glucose followed by incubation at room temperature for 10 min. Uptake was terminated by adding 2 ml ice-cold stop solution (15 mM HEPES buffer (pH 7.6); 135 mM choline Cl; 5 mM KCl; 0.8 mM MgSO4; 1.8 mM $CaCl_2$ and 0.2 mM $HgCl_2$). The cells were rinsed twice with stop solution and lysed in 0.5 ml of 10 mM Tris– HCl (pH 8.0) + 0.2% SDS. Lysed samples were added to 2 ml scintillation cocktail and radio-active emissions determined using a scintillation counter to quantify glucose uptake. For the Uptake Glo luminescent assay uptake was initiated using 2- deoxyglucose solution as per the manufacturer's protocol. Samples were similarly incubated for 10 minutes prior to addition of stop buffer. After neutralisation, the detection reagent was added and luminescence was recorded with 1s integration. For both protocols, all steps took place in the presence or absence of PG (3%), PG:VG (55:45, 3%), Mannitol (7.4%) and/or glucose transport inhibitors phloretin (1 mM dissolved in ethanol) and cytochalasin B (10 μM) or the aquaporin 3 inhibitor (DPF00173, 50μM). Data are presented as % control to normalise between protocols.

Seahorse assay

Human bronchiolar epithelial cells (HBEC) from two independent donors per experiment were seeded into a Seahorse XF96 plate and incubated at 37°C, 5% CO_2 for 48 hours. The medium was changed 24 hours prior to Seahorse experiment and cells were exposed to PG:VG (55:45, 3%), Mannitol (7.4%) for 30 minutes before the Seahorse Glycolysis Stress Assay was performed according to the manufacturer's instructions followed by the sequential injection of oligomycin (1μM) to inhibit ATP-linked respiration and 2-Deoxy-D-Glucose (2-DG; 50mM) to inhibit glucose metabolism. The plate layout was separated into quadrants to reduce edge effects. Extracellular acidification rate (ECAR) and oxygen consumption rate (OCAR) were measured. Glycolysis rate was calculated by subtracting ECAR values after 2-DG injection from the ECAR values after glucose injection in order to exclude the non-glycolytic acidification from the calculation. Glycolytic capacity was calculated by subtracting the non-glycolytic acidification rate (ECAR after 2-DG injection) from the maximum ECAR after 1 μM oligomycin injection.

FRAP

Fluorescence recovery after photobleaching (FRAP) was carried out on human embryonic kidney cells transfected with GLUT1-GFP, GLUT2-mcherry or GLUT10-GFP. HEK293T cells were seeded on #1.5 glass coverslips and transiently transfected with constructs, using Lipofectamine 2000 (Thermo Fisher) as per the manufacturer's instructions. Fluorescence recovery after photobleaching was performed 24–48 hours after transfection, using a Leica SP5 confocal microscope with a 63 × 1.30 numerical aperture glycerol immersion lens as described (25).

Western blots - pMAPK and quantification

Cells were lysed in lysis buffer (50 mM Tris-HCl, pH 7.4; 1% NP-40; 0.25% sodium deoxycholate; 150 mM NaCl; 1 mM EDTA; 1 mM EGTA, 1 mM PMSF, 1 mM Na_3VO_4, 50 mM NaF, 5 mM sodium pyrophosphate and 1% (w/v) Protease inhibitor cocktail). Cellular debris was removed by centrifugation at 13,000x g for 10 minutes and protein concentrations were determined using the Bradford assay (as above) Approximately 30-50µg of proteins were fractionated on 4-12% Bis-tris gel (Invitrogen, Paisley, UK) alongside prestained protein standards (Santa Cruz, CA, USA) and transferred onto Hybond-P PVDF Membrane (GE Healthcare, Amersham, UK). Membranes were incubated in TBS-T containing 5% (w/v) non-fat milk powder for 1 h at room temperature prior to incubation with primary antibodies; anti-phospho-p38 MAPK (Thr180/Tyr182) Antibody #9211 or anti-p38 MAPK #9212 (Cell Signaling Technology, USA) (all diluted 1:1000) followed by incubation with species-specific horseradish peroxidase conjugated secondary antisera (Sigma, UK).

Immunostained proteins were visualized with SuperSignal west pico chemiluminescent substrate (GE Healthcare, Amersham, UK). Densitometric quantification was performed using Scion Image (NIH, USA).

Cytotoxicity

Cytotoxicity was measured by analysing lactate dehydrogenase release from cells using an LDH cytotoxicity assay (Peirce, UK) and cell proliferation was analysed using the CyQUANT® Direct Cell Proliferation Assay according to the manufacturer's instructions. Assays were carried out 30 minutes after exposure to treatments as described above.

Statistical Analysis

For statistical analysis, $P \leq 0.05$ was taken as significant. Data were analysed by ANOVA with post hoc Tukey's/Bonferroni test where indicated. Data are shown as mean ± SE, where n = the number of independent experiments (cell lines) or replicates/measurements from primary cells where the number of donors are stated.

Results

PG and PG/VG inhibits glucose transport

In airway cells the primary route for glucose uptake is via GLUT transporters (23). Glucose transport is often higher in proliferating cells to support cellular growth and particularly in immortalised cell lines such as H441 airway cells. Furthermore, when airway cells are grown at air-liquid interface, glucose transporters are differentially segregated to apical and basolateral domains (22, 29, 37). Therefore we firstly investigated the effect of exposure to PG on glucose uptake in proliferating H441 cells grown on plastic. PG inhibited glucose uptake in a dose dependent manner with 263mM, (equivalent to 3% PG w/v) inhibiting glucose uptake to less than 50% of control. Figure 1A and B.

.

.

We then investigated the effect of exposure to 3% PG and 3% PG/VG 55:45 (a common mix in electronic cigarettes) for 15 minutes in both proliferating H441 and BMI-1 transduced HBEC (which have extended passage potential whilst retaining the characteristics of primary cells). 3% PG and 3% PG/VG inhibited glucose uptake in proliferating H441 and BMI-1

transduced HBEC to 46 ± 23% and 45 ± 17% respectively of control, $p<0.001$, n = 18. Phloretin which blocks GLUT mediated glucose transport had a more potent effect reducing glucose uptake to 13± 1% of control.(23)The effect of 3% PG/VG was not additive to that of phloretin, Figure 1C. In addition, the effect of 3% PG/VG was not additive to the effect of an alternative GLUT transport inhibitor Cytochalasin B (10μM). Glucose transport was reduced to 54 ± 13% and 45 ± 15%, n = 12, respectively (Figure 1C). These data indicate that PG/VG inhibited glucose uptake via GLUT transporters.

3% PG, 3% PG/VG and phloretin had a similar effect on proliferating BMI-1 transduced HBEC, reducing glucose uptake to 54 ± 12%, 56 ± 10% and 15 ± 5% respectively, $p< 0.001$, n=6. Figure 1D.

Exposure to 3% PG/VG reduced glucose transport maximally at 4 hour reaching levels that were similar to that of the glucose transport inhibitor phloretin. However, glucose transport recovered to approximately 50% of control at 24 hours. Figure 1E.

Glucose transport is one of the rate limiting steps of intracellular glucose metabolism and therefore we investigated the effect of PG and PG/VG on glycolysis and mitochondrial ATP generation. As exposure to PG and PG/VG can elicit osmotic effects (31), we also compared their effect to that of exposure to mannitol 7.4% which was isosmolar with PG/VG with a calculated osmolarity of 408.5 mOsm.

PG and PG/VG modify airway cell glucose metabolism

Having demonstrated that PG and PG/VG reduced glucose uptake in BMI-1 transduced HBEC, we then used primary HBEC, from a total of 4 independent donors, to investigate effects on

metabolism by measuring oxygen consumption rate; OCR and extracellular acidification rate; ECAR after the sequential addition of D-glucose (10 mM), oligomycin (1μM) and 2-D-deoxyglucose (50mM) (Figure 2A&B). 3% PG, 3% PG/VG and iso-osmotic mannitol all significantly reduced mitochondrial ATP generation (measured as oxygen consumption rate; OCR) in these airway cells compared to control, $p<0.001$, n = 72, 71 and 66 replicates respectively) (Figure 2 C). Compared to control, PG/VG and mannitol, but not PG, reduced glycolytic capacity ($p<0.0001$, n = 71 and 66 replicates respectively) and glycolytic reserve ($p<0.0001$, n=66) (Figure 2E&F). Only PG/VG inhibited glycolysis ($p<0.001$, n= 71). This indirect evidence raises the possibility that VG mediated the inhibition of glycolysis (Figure 2D). ECAR/OCR after glucose or oligomycin injection reflected the differential effects of PG, PV/VG and mannitol on glycolytic parameters and mitochondrial ATP generation. Figures 2G&H. There was no effect of exposure to 3% PG and 3% PG/VG on cell proliferation or lactate dehydrogenase (LDH) release indicating no initial toxicity. However, exposure to iso-osmolar mannitol significantly reduced cell proliferation to 68 ± 2% of control ($p<0.0001$, n= 11 replicates) and increased LDH release to 122 ± 1% compared to control ($P<0.05$, n=3 replicates). Figures 3A & B.

PG/VG reduced cell surface area

To examine effects on cell surface area we used HEK293 epithelial cells because of their size and suitability for imaging. Exposure to 3% PG/VG or iso-osmolar mannitol rapidly (within 20 seconds) reduced cell surface area (by -9.2±2.4% and -20.4±2.3%, compared to control, -1.4±0.3%, $p<0.01$ and 0.0001, n=7 respectively), indicating cell shrinkage consistent with a hyperosmotic effect. (Figure 4 A & B). Phosphorylation of p38 mitogen activated protein kinase (MAPK) which is associated with osmotic stress was only elevated after exposure to mannitol (reaching a maximum at 30 minutes, $p<0.0001$, $F(1,24) = 24.69$) and not PG/VG

consistent with its more potent effect (Figure 4 C &D). These data indicate that the effect of PG/VG on glucose transport and metabolism is not via activation of p38 MAPK.

PG/VG reduced airway epithelial height, decreased transepithelial resistance, increased epithelial permeability and ASL height.

To better model the *in vivo* airway we investigated the effect of mucosal PG/VG on differentiated HBEC grown at air-liquid-interface (ALI) on permeable supports. Apical application of 3% PG/VG and mannitol initiated a rapid reduction in HBEC cell height from 28.7±2.9 and 30.5±1.5 μm to 21.7±5.7 and 20.6±4.2 respectively ($p<0.001$, n=10 measurements from 3 independent donors). Cell height initially recovered at approximately 10 minutes but then exhibited a continual decline to 90 minutes (Figure 5A and B). Consistent with an apical osmotic challenge, airway surface liquid (ASL) height rapidly increased from 9±2 to 73±18 and 54±16, $p<0.001$, n=10 respectively after 2 minutes and remained elevated up to 10 minutes. ASL then slowly declined but did not reach initial levels even after 90 minutes (Figure 5C). In parallel, apical exposure to 3% PG/VG resulted in a greater decrease in HBEC TEER from 1142±433 to 685±309 $\Omega.cm^2$ than cells exposed to apical iso-osmotic mannitol 920±169 $\Omega.cm^2$, $p<0.05$, n=4 independent donors. Repeated measurement of transepithelial electrical resistance (TEER) causes a decrease over time. However, similar apical exposure of H441 cells to 3% PG/VG resulted in a more rapid and greater decrease in TEER than in cells exposed to apical iso-osmotic mannitol (0-15 minutes, from 348±33 to 209±22 and 347±31 to 258±22 $\Omega.cm^2$ respectively, $p<0.05$, n=15). The additional reduction in TEER was sustained over a period of 24 hours (Figure 5D). The decrease in resistance correlated with an increase in apical to basolateral permeability of the epithelial monolayer to Na^+ fluorescein measured over 90 minutes (Figure 5E). These data indicate that PG/VG induces

effects on cell volume consistent with hyperosmotic effects and additional detrimental effects on airway epithelial barrier function.

PG/VG decreases FRAP of GLUT transporters in the membrane

We then investigated the effect of 3% PG/VG and mannitol on the turnover/movement of GLUT transporters in the cell membrane using fluorescence recovery after photobleaching (FRAP) in HEK293 cells. We investigated GLUT1, 2 and 10 which have all be proposed to play a role in glucose uptake in airway cells. Exposure to 3% PG/VG or mannitol significantly reduced recovery of fluorescence of GLUT1-GFP and GLUT10-GFP expressed in the membrane domain compared to control ($p<0.001$, n=10 independent cell recordings). FRAP of GLUT2-mcherry was less affected by either 3% PG/VG or mannitol. These data indicate that exposure to PG/VG and mannitol reduce glucose uptake in airway cells via mechanisms that reduce the turnover and function of glucose transporters at the membrane. Figures 6A-F.

PG/VG vaped onto the apical surface of HBEC decreases glucose transport

Finally, to more physiologically mimic the way e.cigarette vapour reaches the epithelium, we investigated the effect of 3% PG/VG vaped/puffed onto the apical surface of differentiated HBEC grown at ALI at 27 puffs/10 minutes on cell height. The reduction of cell height was slower but of similar magnitude (from 27±5 to 20±4 μm) (Figure 7A) to that after direct application of PG/VG (see Figure 5B).

A similar treatment of 3% PG/VG puffed onto the apical surface of HBEC mildly reduced basolateral glucose uptake to 84±5% compared to puffing with air alone ($p<0.05$, n=8 from 4 independent donors). Air with basolaterally applied phloretin inhibited to 29±3% of control consistent with previous observations. The effect of 3% PG/VG on apical glucose uptake was

not statistically significant. Phloretin inhibited apical glucose uptake to only 60 ± 9% of control ($p<0.05$, n=4 from 4 independent donors).

Discussion

There is increasing evidence that exposure to e-cigarette vapour induces toxicity, oxidative stress, and inflammatory responses in lung epithelial and endothelial cells (26). Toxicity associated with flavourings have been described (19, 40, 42) as have the effects of nicotine (11, 13). However, less is known about the effects of PG and PG/VG. As it was reported that PG/VG reduced cell growth (19, 42), we set out to investigate whether PG and PG/VG affected glucose uptake and metabolism in airway cells as a potential mechanism for growth inhibition.

Our data are the first to show that a short-term exposure to PG or PG/VG at concentrations comparable to those used in *in vitro* studies as a model of lung exposure (3% w/v), inhibited glucose uptake and suppressed mitochondrial ATP production in airway cells. The dose dependency of PG on glucose uptake and metabolism was consistent with that described in renal cells (31-34). Similar to our observations, PG was shown to inhibit Na+-independent, GLUT mediated glucose uptake in renal cells. We also found evidence that 3% PG/VG inhibited glycolysis. As thiswas not observed with PG only, it is possible that VG mediated this effect. Further work is now required to see if this is indeed the case. Importantly, even in the context of a single exposure to e.cigarette vapour, a decrease in glucose uptake across the serosal membrane highlighted the potency and ability of PG/VG to affect even compartmentalized function of the airway epithelium.

The mechanisms underlying the effects we observed are complex. The addition of sugar alcohols/polyols increases the osmolality of solutions. In this study, we maintained the osmolality of the mannitol, PG and PG/VG solutions at ~408 mOsm (hyperosmotic). Our

finding that these solutions induced rapid changes to HEK293 cell surface area, cell height and ASL height in HBEC indicate hyperosmotic effects on cell volume and a potential link to reduced glucose uptake and metabolism. Such pathways have been reported. Hyperosmotic stress was proposed to decrease ATP synthesis in HT22 nerve cells (14) and exposure to hyperosmotic mannitol in the rat jejenum decreased glucose uptake [26].

Mannitol (which inhaled is used to test airway hyperresponsiveness (7)) also induced a potent phosphorylation of p38 MAPK, typical of classical signalling in osmotic stress (8, 16, 54) Phosphorylation of p38 MAPK in response to osmotic stress has previously been demonstrated in both HEK293 and human airway cells (54). Phosphorylation of p38 MAPK regulates gene expression of key cellular processes such as proliferation and apoptosis. Activation of p38 MAPK was also important for rebalancing the cells energy status, post osmotic insult, by induction of GLUT1 expression in cardiomyocytes and rat liver clone 9 cells but only after more prolonged exposure (12 hours) (10, 16, 21, 44).

Surprisingly, PG/VG did not activate p38 MAPK (and exposure of airway cells previously to PG/VG did not elicit a rise in intracellular Ca^{2+} (42)). We have not yet investigated activation of other signalling pathways (e.g. AMPK which induced glucose uptake in Clone 9 cells, preadipocytes and myoblasts (1)). Nevertheless, the ability of PG/VG to induce similar cell volume changes without inducing phosphorylation of p38 MAPK raises the possibility that adaptation to PG/VG insult is different and could have consequences for cell survival. Certainly, over a longer time course 3% PG/VG was reported to reduce the viability of airway cells (41, 42).

In previous studies, 3% PG/VG produced a decrease in the fluorescence of Merocyanine 540 (M540) incorporated into the plasma membrane of HBEC, indicating an increase in molecular packing stress and reduction of membrane fluidity (19, 25). Mannitol induced cell shrinkage would also result in increased surface packing of membrane lipids and a reduction in membrane fluidity. Such a reduction in membrane fluidity would provide a mechanism for the reduced recovery of facilitative GLUT transporters we observed in the membrane of airway cells after photobleaching. In particular, FRAP of GLUT1 and GLUT10 were potently reduced. GLUT1 is ubiquitous and the primary route for glucose uptake in proliferating cells and it has been demonstrated on the basolateral membrane of differentiated HBEC (37). GLUT10 has been observed in the apical membrane domain of H441 cells and HBEC, but its role in glucose uptake in the airway is not well understood and it may have additional roles as a mitochondrial transporter (2, 3, 17, 22, 23). Both transporters have a higher affinity for glucose than GLUT2 which was modestly affected (K_m ~3mM, ~0.3 mM and 17mM respectively). Thus, under normal culture and experimental conditions where glucose concentration is 5-10mM, although we cannot rule out competitive inhibition of glucose transport by PG or PG/VG, the effect of membrane packing stress and reduced diffusibility of GLUT1 and 10 would likely suppress glucose transport and consequently glucose metabolism during the hyperosmotic insult.

PG/VG also induced a rapid decrease in TEER in H441 airway cells but mannitol did not. Interestingly, mannitol did not cause a decrease in TEER in differentiated 16HBE14o- airway cells when osmolarity was below 450mOsm (36). Unlike mannitol, PG and VG can permeate membranes and high VG concentration was shown to modify membrane structure not only by osmotic volume contraction but also by direct interactions with the lipid components in the membrane (5, 6, 27). Such interaction with the plasma membrane is likely to produce detrimental effects on the tight junctions between airway epithelial cells causing the decrease

in TEER and subsequent increase in transepithelial permeability. In support of this notion, glycerol was shown to disrupt tight junction-associated proteins F-actin, occludin and tubulin organization in rat Sertoli cells. A derivative of PG, propylene glycol caprylate, also decreased intestinal epithelial TEER via effects on tight junction proteins including occludin and ZO-1, which are present in airway cells (18, 24, 48, 49). We did not investigate effects on ASL height beyond 90 minutes, but a sustained loss of barrier function, as seen in H441 cells, would likely result in an inability to regulate airway surface liquid volume and disrupt innate immune function of the airway and predispose to infection (27, 28, 51, 52).

In conclusion, we show that short term exposure to PG and VG, key components of e-cigarettes, either in solution or vaped on the luminal surface of airway cells, decreased GLUT mediated glucose transport and ATP production in airway cells. We propose that this occurred as a result of changes to cell volume and membrane fluidity caused by osmotic effects and direct interaction of PG/VG with lipids in the cell membrane. PG/VG also decreased barrier function and increased epithelial permeability. Taken together, we suggest that all these factors contribute to reduced defensive properties of the epithelium which could lead to increased susceptibility of the lungs to infection. We propose that repeated/chronic exposure to these agents are likely to contribute to airway damage in e-cigarette users.

Acknowledgements

M.W. was funded with a The Cystic Fibrosis Trust studentship, J.J. was funded by St George's, University of London, K.K. was funded by Astra Zeneca, Gothenburg, Sweden. J.P.G. was funded by a Respiratory Diseases Research Award from the Medical Research Foundation (MRF-091-0001-RG-GARNE) and R.T. was funded by NIH/NHLBI HL135642.

References

1. **Abbud W, Habinowski S, Zhang JZ, Kendrew J, Elkairi FS, Kemp BE, Witters LA, and Ismail-Beigi F**. Stimulation of AMP-activated protein kinase (AMPK) is associated with enhancement of Glut1-mediated glucose transport. *Arch Biochem Biophys* 380: 347-352, 2000.
2. **Baines DL, and Baker EM**. Glucose Transport and Homeostasis in Lung Epithelia. *in Lung Epithelial Biology in the Pathogenesis of Pulmonary Disease Eds Sidhaye, V K and Koval, M Oxford: Academic Press* pp. 33-58., 2017.
3. **Baker EH, and Baines DL**. Airway Glucose Homeostasis: A New Target in the Prevention and Treatment of Pulmonary Infection. *Chest* 2017.
4. **Bedichek E, and Kirschbaum B**. A case of propylene glycol toxic reaction associated with etomidate infusion. *Arch Intern Med* 151: 2297-2298, 1991.
5. **Biondi AC, and Disalvo EA**. Effect of glycerol on the interfacial properties of dipalmitoylphosphatidylcholine liposomes as measured with merocyanine 540. *Biochim Biophys Acta* 1028: 43-48, 1990.
6. **Biondi AC, Feliz MR, and Disalvo EA**. Surface changes induced by osmotic stress and its influence on the glycerol permeability in lipid bilayers. *Biochim Biophys Acta* 1069: 5-13, 1991.
7. **Brannan JD, Anderson SD, Perry CP, Freed-Martens R, Lassig AR, Charlton B, and Aridol Study G**. The safety and efficacy of inhaled dry powder mannitol as a bronchial provocation test for airway hyperresponsiveness: a phase 3 comparison study with hypertonic (4.5%) saline. *Respir Res* 6: 144, 2005.
8. **Brocker C, Thompson DC, and Vasiliou V**. The role of hyperosmotic stress in inflammation and disease. *Biomol Concepts* 3: 345-364, 2012.
9. **Choi HC, Kim CS, and Tarran R**. Automated acquisition and analysis of airway surface liquid height by confocal microscopy. *Am J Physiol Lung Cell Mol Physiol* 309: L109-118, 2015.
10. **Chukwuma C, Matsabisa M, Erukainurea O, Ibejic C, and Islam S**. D-mannitol modulates glucose uptake ex vivo; suppresses intestinal glucose absorption in normal and type 2 diabetic rats. *Food Bioscience*

29: 30-36, 2019.
11. **Chung S, Baumlin N, Dennis JS, Moore R, Salathe SF, Whitney PL, Sabater J, Abraham WM, Kim MD, and Salathe M**. Electronic Cigarette Vapor with Nicotine Causes Airway Mucociliary Dysfunction Preferentially via TRPA1 Receptors. *Am J Respir Crit Care Med* 200: 1134-1145, 2019.
12. **Clunes LA, Davies CM, Coakley RD, Aleksandrov AA, Henderson AG, Zeman KL, Worthington EN, Gentzsch M, Kreda SM, Cholon D, Bennett WD, Riordan JR, Boucher RC, and Tarran R**. Cigarette smoke exposure induces CFTR internalization and insolubility, leading to airway surface liquid dehydration. *Faseb J* 26: 533-545, 2012.
13. **Crotty Alexander LE, Drummond CA, Hepokoski M, Mathew D, Moshensky A, Willeford A, Das S, Singh P, Yong Z, Lee JH, Vega K, Du A, Shin J, Javier C, Tian J, Brown JH, and Breen EC**. Chronic inhalation of e-cigarette vapor containing nicotine disrupts airway barrier function and induces systemic inflammation and multiorgan fibrosis in mice. *Am J Physiol Regul Integr Comp Physiol* 314: R834-R847, 2018.
14. **Dafre AL, Schmitz AE, and Maher P**. Hyperosmotic Stress Initiates AMPK-Independent Autophagy and AMPK- and Autophagy-Independent Depletion of Thioredoxin 1 and Glyoxalase 2 in HT22 Nerve Cells. *Oxid Med Cell Longev* 2019: 2715810, 2019.
15. **Davis ES, Sassano MF, Goodell H, and Tarran R**. E-Liquid Autofluorescence can be used as a Marker of Vaping Deposition and Third-Hand Vape Exposure. *Sci Rep* 7: 7459, 2017.
16. **Galvez AS, Ulloa JA, Chiong M, Criollo A, Eisner V, Barros LF, and Lavandero S**. Aldose reductase induced by hyperosmotic stress mediates cardiomyocyte apoptosis: differential effects of sorbitol and mannitol. *J Biol Chem* 278: 38484-38494, 2003.

17. **Garnett JP, Baker EH, and Baines DL**. Sweet talk: insights into the nature and importance of glucose transport in lung epithelium. *Eur Respir J* 40: 1269-1276, 2012.
18. **Garnett JP, Gray MA, Tarran R, Brodlie M, Ward C, Baker EH, and Baines DL**. Elevated paracellular glucose flux across cystic fibrosis airway epithelial monolayers is an important factor for Pseudomonas aeruginosa growth. *PLoS One* 8: e76283, 2013.
19. **Ghosh A, Coakley RC, Mascenik T, Rowell TR, Davis ES, Rogers K, Webster MJ, Dang H, Herring LE, Sassano MF, Livraghi-Butrico A, Van Buren SK, Graves LM, Herman MA, Randell SH, Alexis NE, and Tarran R**. Chronic E-cigarette Exposure Alters the Human Bronchial Epithelial Proteome. *Am J Respir Crit Care Med* 2018.
20. **Harvanko A, Kryscio R, Martin C, and Kelly T**. Stimulus effects of propylene glycol and vegetable glycerin in electronic cigarette liquids. *Drug Alcohol Depend* 194: 326-329, 2019.
21. **Hwang DY, and Ismail-Beigi F**. Stimulation of GLUT-1 glucose transporter expression in response to hyperosmolarity. *Am J Physiol Cell Physiol* 281: C1365-1372, 2001.
22. **Kalsi KK, Baker EH, Fraser O, Chung YL, Mace OJ, Tarelli E, Philips BJ, and Baines DL**. Glucose homeostasis across human airway epithelial cell monolayers: role of diffusion, transport and metabolism. *Pflugers Arch* 457: 1061-1070, 2009.
23. **Kalsi KK, Baker EH, Medina RA, Rice S, Wood DM, Ratoff JC, Philips BJ, and Baines DL**. Apical and basolateral localisation of GLUT2 transporters in human lung epithelial cells. *Pflugers Arch* 456: 991-1003, 2008.
24. **Kalsi KK, Garnett JP, Patkee W, Weekes A, Dockrell ME, Baker EH, and Baines DL**. Metformin attenuates the effect of Staphylococcus aureus on airway tight junctions by increasing PKCzeta-mediated phosphorylation of occludin. *J Cell Mol Med* 23: 317-327, 2019.
25. **Langner M, and Hui SW**. Merocyanine 540 as a fluorescence indicator for molecular packing stress at the onset of lamellar-hexagonal transition of phosphatidylethanolamine bilayers. *Biochim Biophys Acta* 1415: 323-330, 1999.
26. **Lerner CA, Sundar IK, Yao H, Gerloff J, Ossip DJ, McIntosh S, Robinson R, and Rahman I**. Vapors produced by electronic cigarettes and e-juices with flavorings induce toxicity, oxidative stress, and inflammatory response in lung epithelial cells and in mouse lung. *PLoS One* 10: e0116732, 2015.
27. **Madison MC, Landers CT, Gu BH, Chang CY, Tung HY, You R, Hong MJ, Baghaei N, Song LZ, Porter P, Putluri N, Salas R, Gilbert BE, Levental I, Campen MJ, Corry DB, and Kheradmand F**. Electronic cigarettes disrupt lung lipid homeostasis and innate immunity independent of nicotine. *J Clin Invest* 129: 4290-4304, 2019.
28. **Miyashita L, Suri R, Dearing E, Mudway I, Dove RE, Neill DR, Van Zyl-Smit R, Kadioglu A, and Grigg J**. E-cigarette vapour enhances pneumococcal adherence to airway epithelial cells. *European Respiratory Journal* 51: 2018.
29. **Molina SA, Moriarty HK, Infield DT, Imhoff BR, Vance RJ, Kim AH, Hansen JM, Hunt WR, Koval M, and McCarty NA**. Insulin signaling via the PI3K/Akt pathway regulates airway glucose uptake and barrier function in a CFTR-dependent manner. *Am J Physiol Lung Cell Mol Physiol* ajplung 00364 02016, 2017.
30. **Morshed KM, Jain SK, and McMartin KE**. Acute toxicity of propylene glycol: an assessment using cultured proximal tubule cells of human origin. *Fundam Appl Toxicol* 23: 38-43, 1994.
31. **Morshed KM, Jain SK, and McMartin KE**. Propylene glycol-mediated cell injury in a primary culture of human proximal tubule cells. *Toxicol Sci* 46: 410-417, 1998.
32. **Morshed KM, L'Helgoualch A, Nagpaul JP, Amma MK, and Desjeux JF**. The role of propylene glycol metabolism in lactatemia in the rabbit. *Biochem Med Metab Biol* 46: 145-151, 1991.
33. **Morshed KM, Nagpaul JP, Majumdar S, and Amma MK**. Kinetics of oral propylene glycol-induced acute hyperlactatemia. *Biochem Med Metab Biol* 42: 87-94, 1989.
34. **Morshed KM, Nagpaul JP, Majumdar S, and Amma MK**. Kinetics of propylene glycol elimination and metabolism in rat. *Biochem Med Metab Biol* 39: 90-97, 1988.

35. **Munye MM, Shoemark A, Hirst RA, Delhove JM, Sharp TV, McKay TR, O'Callaghan C, Baines DL, Howe SJ, and Hart SL**. BMI-1 extends proliferative potential of human bronchial epithelial cells while retaining their mucociliary differentiation capacity. *Am J Physiol Lung Cell Mol Physiol* 312: L258-L267, 2017.
36. **Nilsson H, Dragomir A, Ahlander A, Johannesson M, and Roomans GM**. Effects of hyperosmotic stress on cultured airway epithelial cells. *Cell Tissue Res* 330: 257-269, 2007.
37. **Pezzulo AA, Gutierrez J, Duschner KS, McConnell KS, Taft PJ, Ernst SE, Yahr TL, Rahmouni K, Klesney-Tait J, Stoltz DA, and Zabner J**. Glucose depletion in the airway surface liquid is essential for sterility of the airways. *PLoS One* 6: e16166, 2011.
38. **Pisinger C**. Why public health people are more worried than excited over e-cigarettes. *BMC Med* 12: 226, 2014.
39. **Randell S, Fulcher ML, O'Neal W, and Olsen J**. Primary Epithelial Cell Models for Cystic Fibrosis Research. In: *Cystic Fibrosis*, edited by Amaral MD, and Kunzelmann KHumana Press, 2011, p. 285-310.
40. **Rowell TR, Keating JE, Zorn BT, Glish GL, Shears SB, and Tarran R**. Flavored e-liquids increase cytoplasmic Ca(2+) levels in airway epithelia. *Am J Physiol Lung Cell Mol Physiol* 318: L226-L241, 2020.
41. **Rowell TR, Reeber SL, Lee SL, Harris RA, Nethery RC, Herring AH, Glish GL, and Tarran R**. Flavored e-cigarette liquids reduce proliferation and viability in the CALU3 airway epithelial cell line. *Am J Physiol Lung Cell Mol Physiol* 313: L52-L66, 2017.
42. **Sassano MF, Davis ES, Keating JE, Zorn BT, Kochar TK, Wolfgang MC, Glish GL, and Tarran R**. Evaluation of e-liquid toxicity using an open-source high-throughput screening assay. *PLoS Biol* 16: e2003904, 2018.
43. **Smith TT, Heckman BW, Wahlquist AE, Cummings KM, and Carpenter MJ**. The impact of e-liquid propylene glycol and vegetable glycerin ratio on ratings of subjective effects, reinforcement value, and use in current smokers. *Nicotine Tob Res* 2019.
44. **Sozen B, Ozturk S, Yaba A, and Demir N**. The p38 MAPK signalling pathway is required for glucose metabolism, lineage specification and embryo survival during mouse preimplantation development. *Mech Dev* 138 Pt 3: 375-398, 2015.
45. **Tagalakis AD, Munye MM, Ivanova R, Chen H, Smith CM, Aldossary AM, Rosa LZ, Moulding D, Barnes JL, Kafetzis KN, Jones SA, Baines DL, Moss GWJ, O'Callaghan C, McAnulty RJ, and Hart SL**. Effective silencing of ENaC by siRNA delivered with epithelial-targeted nanocomplexes in human cystic fibrosis cells and in mouse lung. *Thorax* 73: 847-856, 2018.
46. **Tan CD, Smolenski RT, Harhun MI, Patel HK, Ahmed SG, Wanisch K, Yanez-Munoz RJ, and Baines DL**. AMP-activated protein kinase (AMPK)-dependent and -independent pathways regulate hypoxic inhibition of transepithelial Na+ transport across human airway epithelial cells. *Br J Pharmacol* 167: 368-382, 2012.
47. **Tarran R, Sabater JR, Clarke TC, Tan CD, Davies CM, Liu J, Yeung A, Garland AL, Stutts MJ, Abraham WM, Phillips G, Baker WR, Wright CD, and Wilbert S**. Nonantibiotic macrolides prevent human neutrophil elastase-induced mucus stasis and airway surface liquid volume depletion. *Am J Physiol Lung Cell Mol Physiol* 304: L746-756, 2013.
48. **Ukai H, Kawagoe A, Sato E, Morishita M, Katsumi H, and Yamamoto A**. Propylene Glycol Caprylate as a Novel Potential Absorption Enhancer for Improving the Intestinal Absorption of Insulin: Efficacy, Safety, and Absorption-Enhancing Mechanisms. *J Pharm Sci* 2019.
49. **Wiebe JP, Kowalik A, Gallardi RL, Egeler O, and Clubb BH**. Glycerol disrupts tight junction-associated actin microfilaments, occludin, and microtubules in Sertoli cells. *J Androl* 21: 625-635, 2000.
50. **Wieslander G, Norback D, and Lindgren T**. Experimental exposure to propylene glycol mist in aviation emergency training: acute ocular and respiratory effects. *Occup Environ Med* 58: 649-655, 2001.

51. **Wu Q, Jiang D, Minor M, and Chu HW**. Electronic cigarette liquid increases inflammation and virus infection in primary human airway epithelial cells. *PLoS One* 9: e108342, 2014.
52. **Ying KL, Song MA, Weng DY, Nickerson QA, McElroy JP, Brasky TM, Wewers MD, Mathe E, Freudenheim JL, and Shields PG**. Microbial and inflammatory response to electronic cigarette and cigarette use. *Cancer Research* 79: 2019.
53. **Yorgin PD, Theodorou AA, Al-Uzri A, Davenport K, Boyer-Hassen LV, and Johnson MI**. Propylene glycol-induced proximal renal tubular cell injury. *Am J Kidney Dis* 30: 134-139, 1997.
54. **Zhou X, Naguro I, Ichijo H, and Watanabe K**. Mitogen-activated protein kinases as key players in osmotic stress signaling. *Biochim Biophys Acta* 1860: 2037-2052, 2016.

Figure legends

Figure 1. PG and PG/VG inhibit glucose uptake in proliferating airway cells.

Exposure to propylene glycol (PG) (33-263 mM) for 30 minutes decreased glucose uptake shown as % control in a concentration dependent manner in A. H441 and B. BMI-1 transduced HBEC. The inhibition of glucose uptake after a 30 minute exposure to 3% PG (263mM) or 3% PG mixed with vegetable glycerine (PG:VG; 45:55) with and without the GLUT inhibitors phloretin (PT), Cytochalasin B (CB) or PT or CB alone. C. H441 or D. BMI-1 transduced HBEC. E. Exposure of H441 cells to 3% PG:VG; 45:55 (closed circles) decreased glucose uptake in a time dependent manner. The effect of PT (open squares) on glucose transport at 24 hours is shown for reference. Data are shown as box and whisker plots. Horizontal line, median; box, 25-75th percentiles; whiskers, min and max; +, mean. Significantly different from control * $p<0.05$, **$p<0.01$, ***$p<0.001$, ****$p<0.0001$.

Figure 2. PG and PG/VG modify airway cell glucose metabolism.

The effect of 3% PG or 3% PG/VG, 45:55 or isosmotic mannitol on HBEC metabolism. A. Oxygen consumption rate; OCR and B. Extracellular acidification rate; ECAR after sequential addition of glucose, oligomycin and 2-deoxy-D-glucose (2-DG). C. Mitochondrial ATP

production measured as oxidative consumption rate (OCR), D. Glycolysis, E. Glycolytic capacity and F. Glycolytic reserve all measured as extracellular acidification rate (ECAR), G. ECAR/OCR after glucose injection to initiate metabolism and H. ECAR/OCR after oligomycin injection to inhibit oxidative phosphorylation. Data are shown as box and whisker plots. Horizontal line, median; box, 25-75th percentiles; whiskers, min and max; +, mean. Significantly different from control *** $p<0.001$, **** $P<0.0001$.

Figure 3. PG and PG/VG did not inhibit airway cell proliferation or elevate cytotoxic markers.

The effect of 30 minutes exposure to 3% PG or 3% PG/VG, 45:55 or isosmotic mannitol on HBEC A. CyQuant Direct assay of DNA content measured as fluorescence and B. Lactate dehydrogenase (LDH) release measured as absorbance 450-680nM. Data are shown as box and whisker plots. Horizontal line, median; box, 25-75th percentiles; whiskers, min and max; +, mean. Significantly different from control * $p<0.05$, **** $P<0.0001$.

Figure 4. PG/VG decreases cell surface area but does not elevate p38 MAPK

A. Fluorescence microscopy of calcein-AM loaded HEK293 cells before (control) and after exposure to 3% PG/VG or iso-osmotic mannitol. Calcein fluorescent cells are seen as bright white in images. B. Surface area (%), of cells exposed to 3% PG/VG or mannitol (as shown in A), over a time course of 120 seconds. C. Collated data of percent change in surface area (Δ Surface Area %) as shown in B. Data are shown as box and whisker plots. Horizontal line, median; box, 25-75th percentiles; whiskers, min and max; +, mean. D. Western blots of phosphorylated p38 MAPK (p-p38, upper panel) and non-phosphorylated p38 MAPK after

exposure to mannitol or 3% PG/VG for 0-60 minutes. E. Quantification of phospho-p38/total p38MAPK from n=3 experiments. Data are shown as mean ± SD.

Figure 5. PG/VG reduced airway epithelial height, decreased transepithelial resistance, increased epithelial permeability and ASL height

A. Representative fluorescence microscopy images of calcein-AM loaded HBEC (green; for cell height measurement) or rhodamine-dextran labelled airway surface liquid (ASL) overlying HBEC (red; for ASL height measurement) before (control) and after mucosal exposure to 3% PG/VG or mannitol. Effect of control (closed circles), 3% PG/VG (open squares) or iso-osmotic mannitol (closed triangles) on B. Cell height and C. ASL height. D. TEER and E. transepithelial permeability measured across H441 cells grown at air-liquid interface. Dotted lines in B and C represent untreated control levels. Data are shown as mean ± SD. Significantly different from control. * $p<0.05$, ** $p<0.01$, **** $p<0.0001$.

Figure 6. PG/VG decreases FRAP of GLUT transporters.

A. Fluorescence of GLUT1-GFP expressed in HEK293 cells showing areas measured for background, membrane fluorescence and region of interest (ROI) at baseline, after fluorescent photobleaching (Bleach) and recovery. B. GLUT10-GFP and C. GLUT2-mCherry expressed in HEK293 cells. Graphs showing FRAP in control cells (black line) or after treatment with 3% PG/VG (red line) or mannitol (blue line) over a time course of 90 seconds for D. GLUT1-GFP, E. GLUT2-mCherry and F. GLUT10-GFP. Data are shown as mean ± SEM with error bars shown in one direction for clarity. Significantly different from control as shown or *** $p<0.01$, **** $p<0.0001$.

Figure 7. PG/VG vaped onto the apical surface of HBEC decreases glucose transport.

Effect of 3% PG/VG puffed onto mucosal surface (VAPE) of primary HBEC on A. Cell height. Effect of 3% PG/VG (VAPE), or air (AIR) puffed onto mucosal surface or air plus the addition of phloretin (AIR PT) on B. Glucose uptake across the basolateral (serosal) membrane and C. Glucose uptake across the apical (mucosal) membrane. Data are shown as box and whisker plots. Horizontal line, median; box, 25-75th percentiles; whiskers, min and max; +, mean. Significantly different from control as shown or * $p<0.05$, ** $p<0.01$, *** $p<0.001$.

DB, JPG and RT conceived experiments. MW, JJ, VS, DE, KB, KI and KK carried out experiments and data analysis. DB wrote the paper with contributions from JPG and RT.

Figure 1

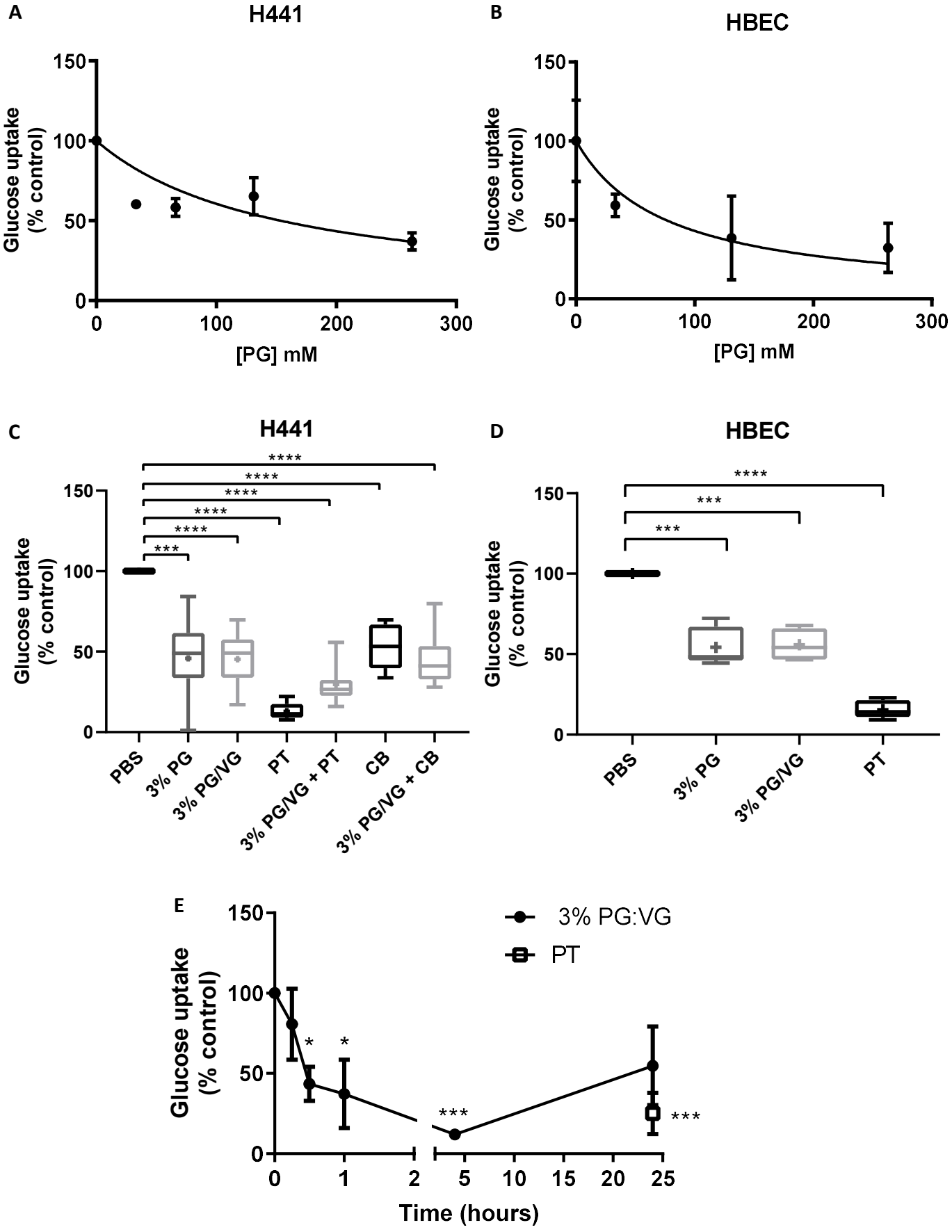
A
H441
Glucose uptake (% control)
150
100
50
0
0
100
200
300
[PG] mM
B
HBEC
Glucose uptake (% control)
150
100
50
0
0
100
200
300
[PG] mM
C
H441
Glucose uptake (% control)
****
****
****
****
****
***
PBS
3% PG
3% PG/VG
PT
3% PG/VG + PT
CB
3% PG/VG + CB
D
HBEC
Glucose uptake (% control)
****
***
***
PBS
3% PG
3% PG/VG
PT
E
Glucose uptake (% control)
3% PG:VG
PT
*
*
***
***
Time (hours)

Figure 2

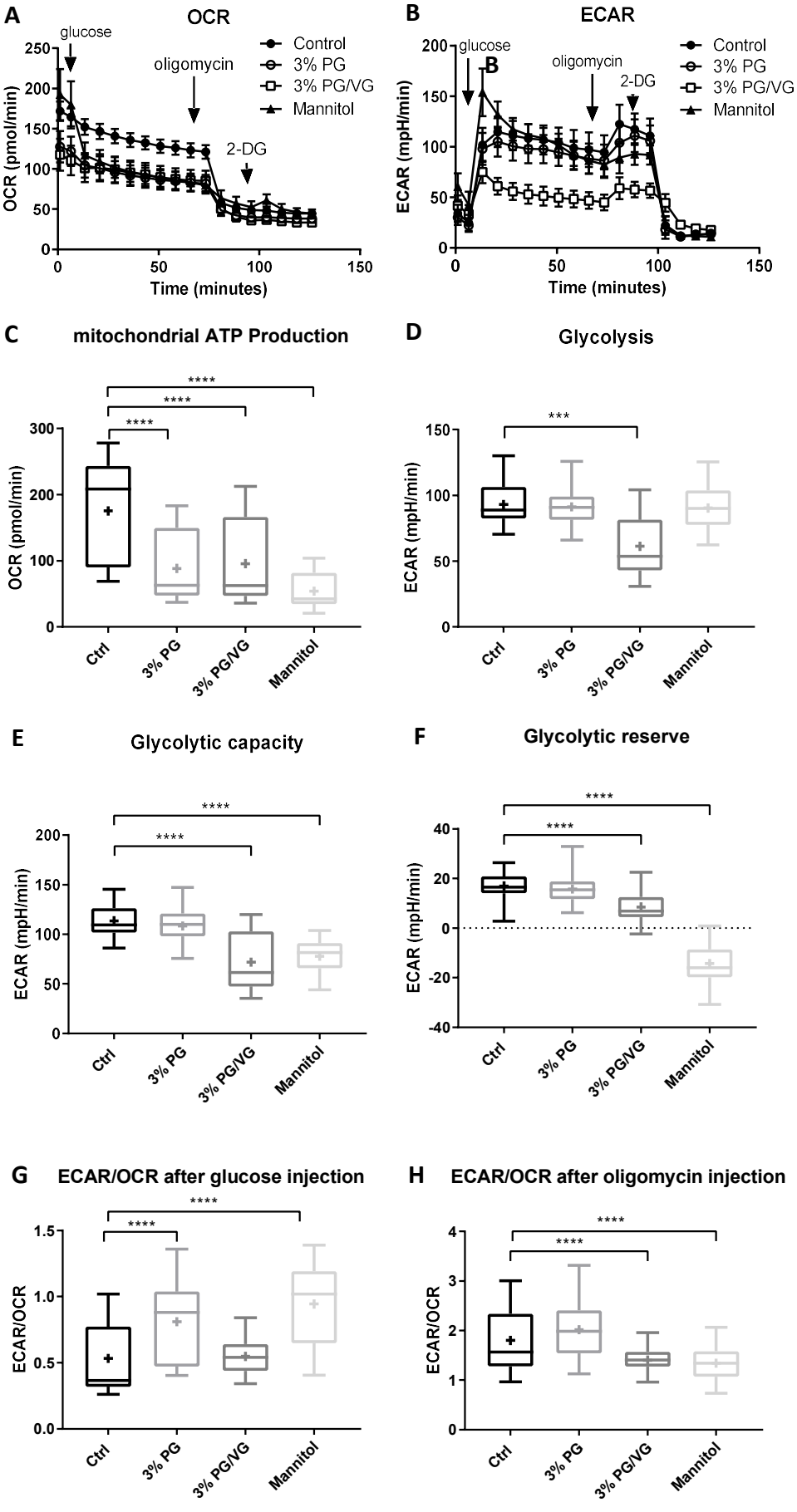
A
OCR
glucose
oligomycin
2-DG
Control
3% PG
3% PG/VG
Mannitol
OCR (pmol/min)
Time (minutes)
B
ECAR
ECAR (mpH/min)
C
mitochondrial ATP Production
D
Glycolysis
E
Glycolytic capacity
F
Glycolytic reserve
G
ECAR/OCR after glucose injection
H
ECAR/OCR after oligomycin injection
Ctrl
3% PG
3% PG/VG
Mannitol

Figure 3

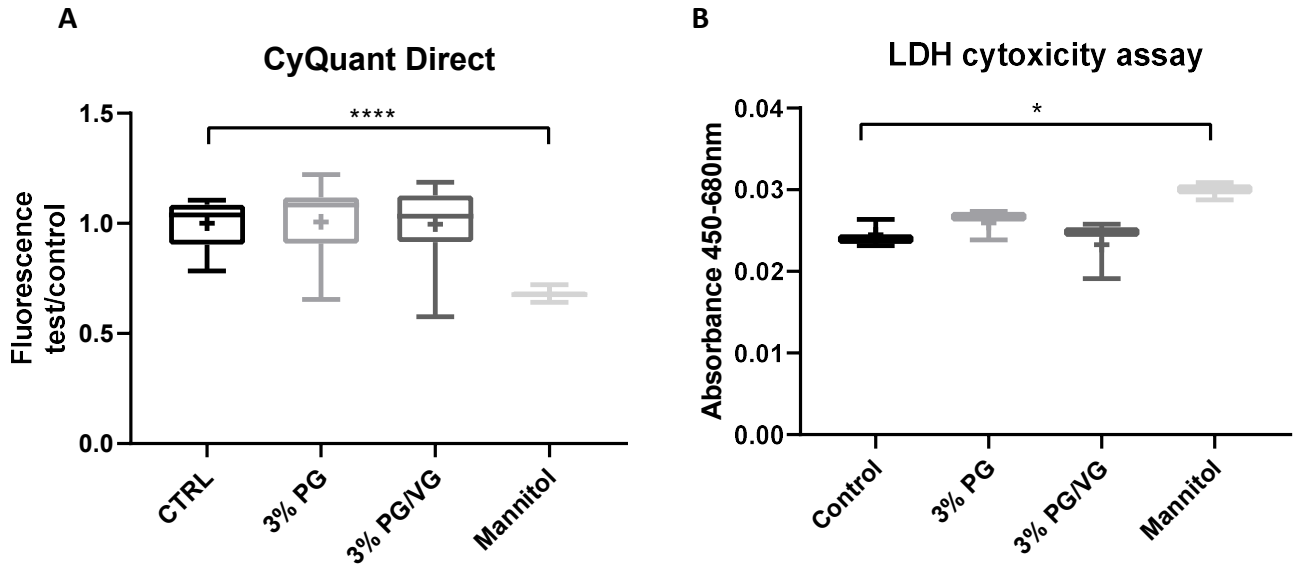
A
CyQuant Direct
****
Fluorescence test/control
1.5
1.0
0.5
0.0
CTRL
3% PG
3% PG/VG
Mannitol
B
LDH cytoxicity assay
*
Absorbance 450-680nm
0.04
0.03
0.02
0.01
0.00
Control
3% PG
3% PG/VG
Mannitol

Figure 4

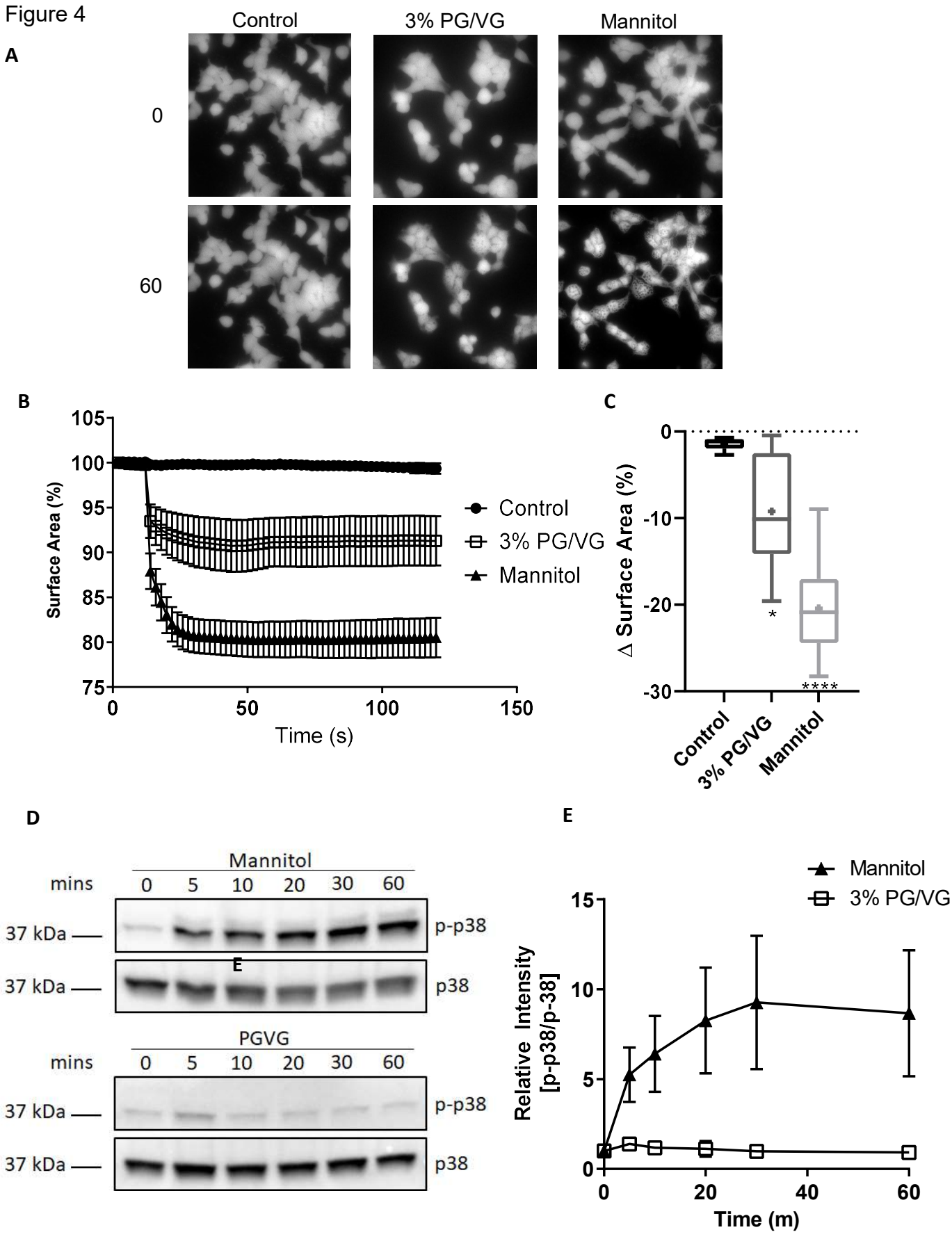
A
Control
3% PG/VG
Mannitol
0
60
B
Surface Area (%)
105
100
95
90
85
80
75
0
50
100
150
Time (s)
Control
3% PG/VG
Mannitol
C
Δ Surface Area (%)
0
-10
-20
-30
*
****
Control
3% PG/VG
Mannitol
D
Mannitol
mins
0 5 10 20 30 60
37 kDa
p-p38
37 kDa
p38
PGVG
mins
0 5 10 20 30 60
37 kDa
p-p38
37 kDa
p38
E
Mannitol
3% PG/VG
Relative Intensity [p-p38/p-38]
15
10
5
0
0
20
40
60
Time (m)

Figure 5

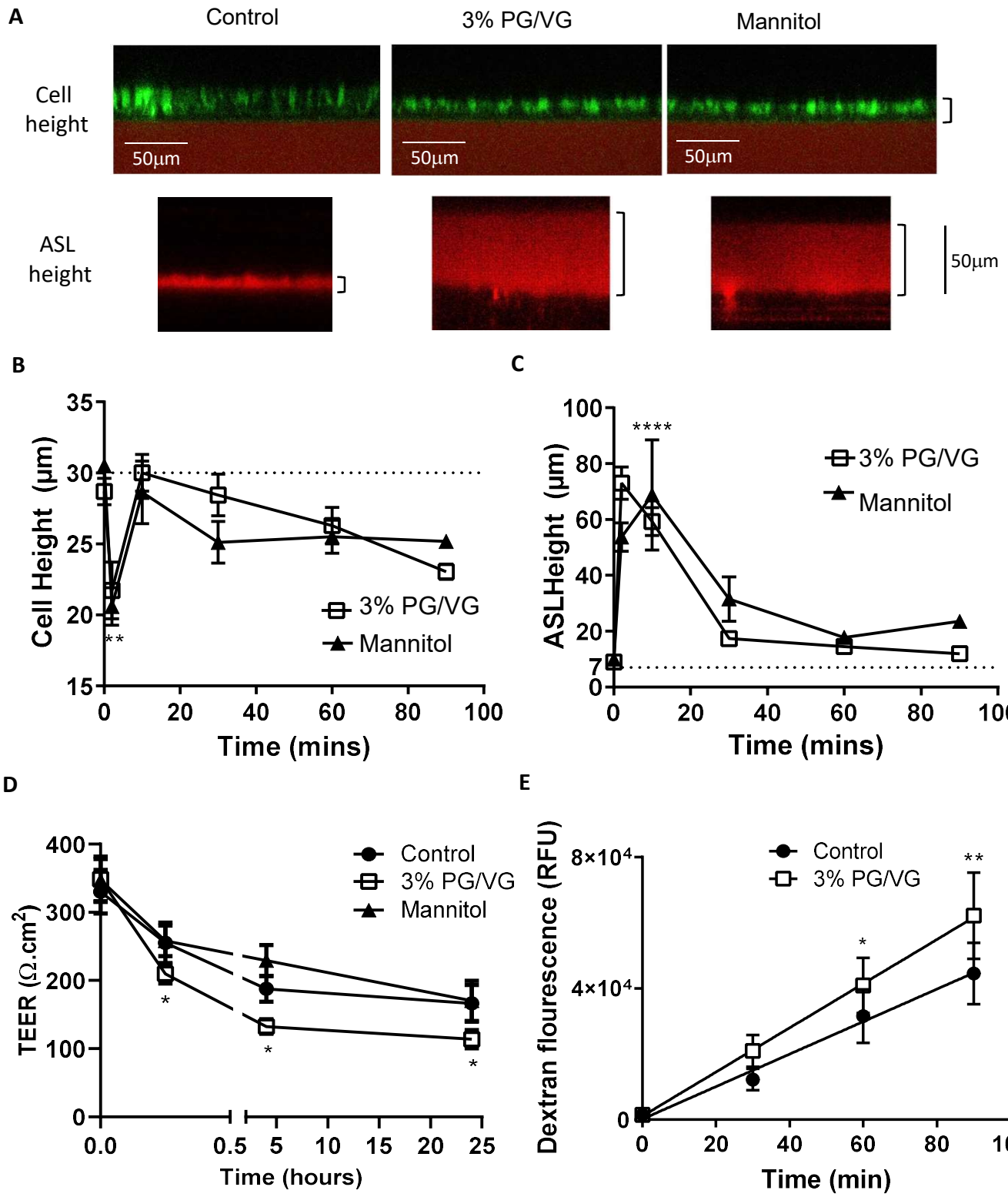
A
Control
3% PG/VG
Mannitol
Cell height
ASL height
50µm
B
Cell Height (µm)
Time (mins)
3% PG/VG
Mannitol
C
ASLHeight (µm)
Time (mins)
****
D
TEER (Ω.cm²)
Time (hours)
Control
3% PG/VG
Mannitol
E
Dextran flourescence (RFU)
Time (min)
Control
3% PG/VG

Figure 6

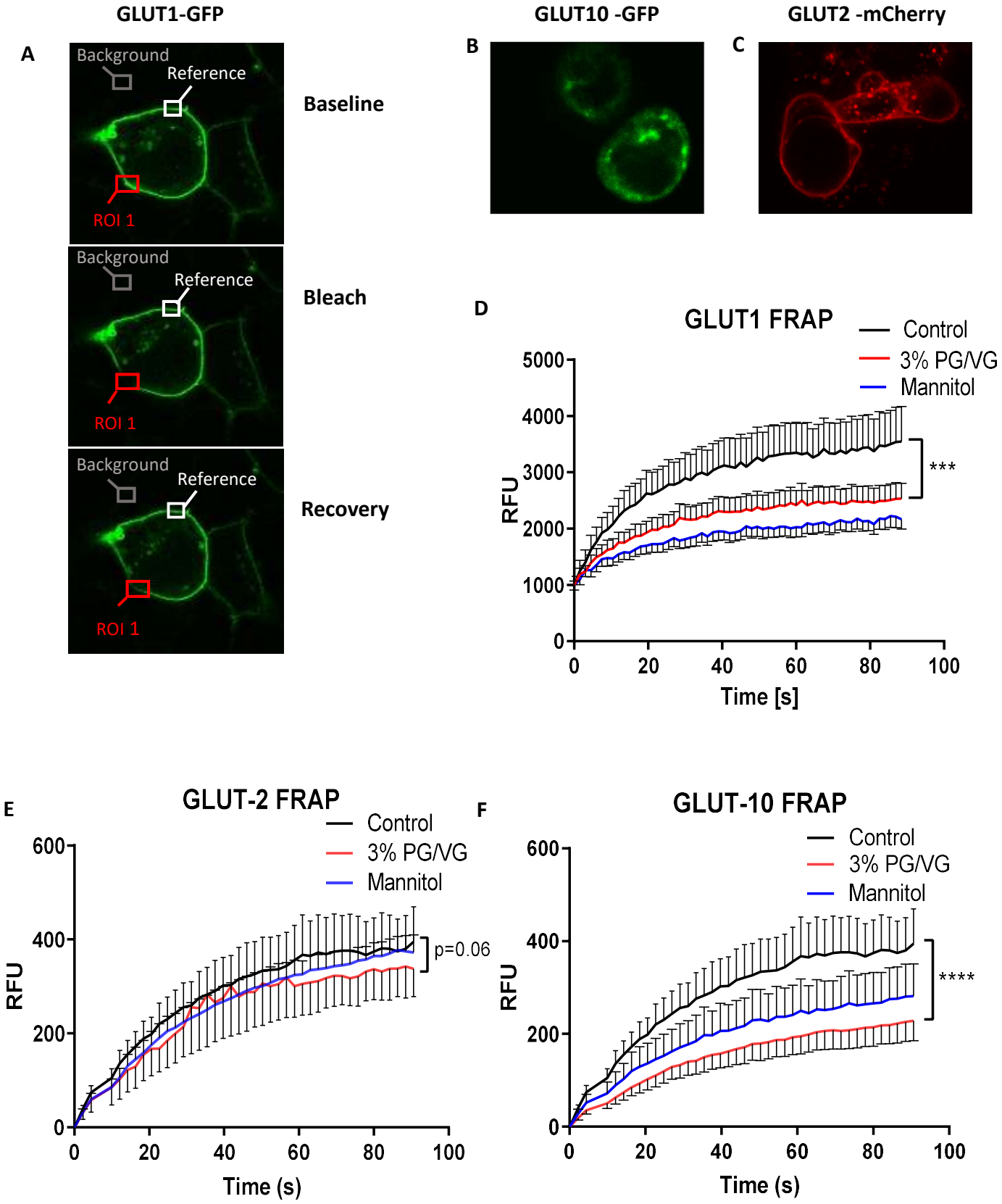
GLUT1-GFP
A
Background
Reference
ROI 1
Baseline
Bleach
Recovery
B
GLUT10 -GFP
C
GLUT2 -mCherry
D
GLUT1 FRAP
Control
3% PG/VG
Mannitol
RFU
Time [s]
***
E
GLUT-2 FRAP
p=0.06
Time (s)
F
GLUT-10 FRAP
****
Time (s)

Figure 7

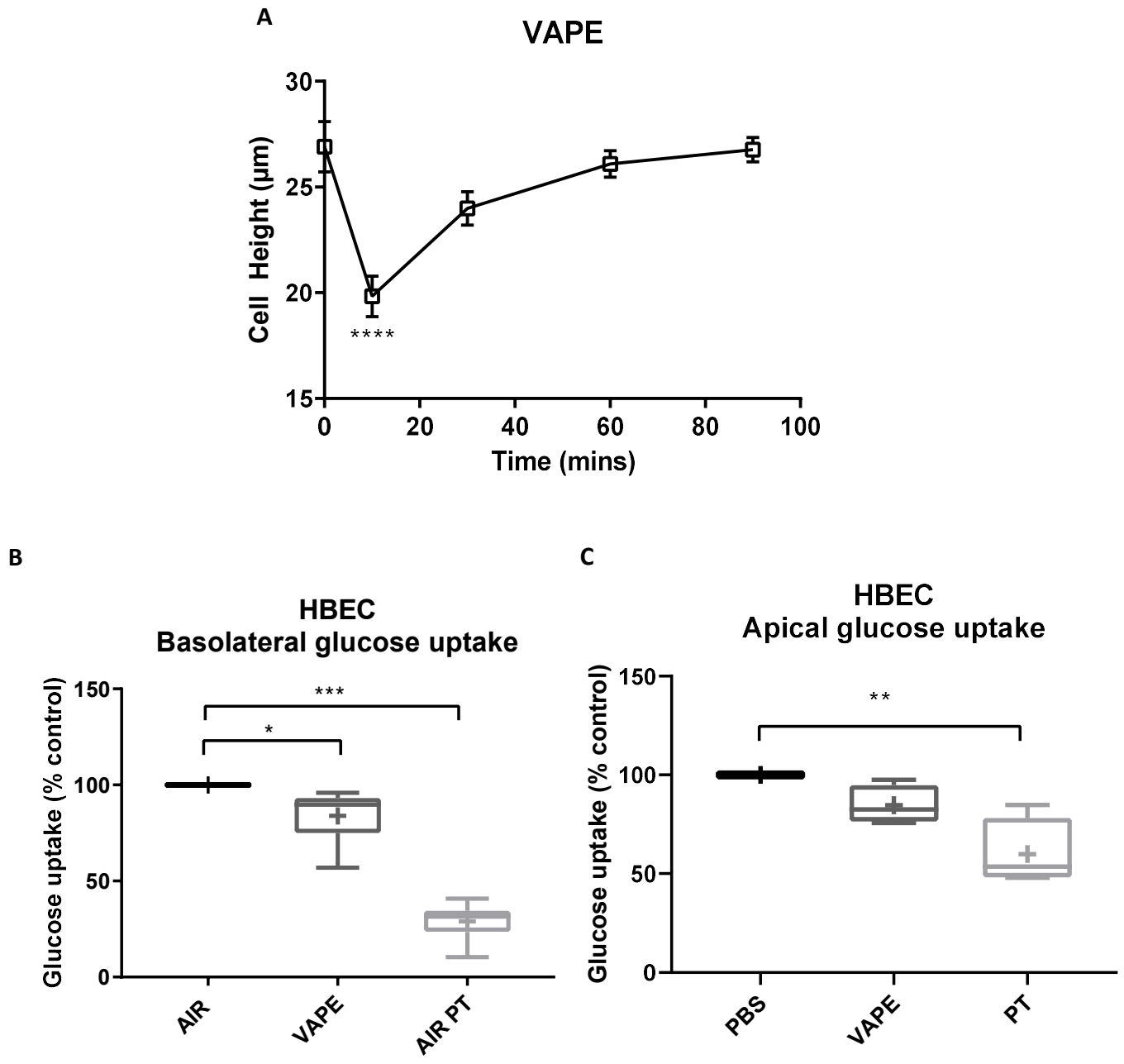
A
VAPE
Cell Height (µm)
30
25
20
15
****
0
20
40
60
80
100
Time (mins)
B
HBEC
Basolateral glucose uptake
Glucose uptake (% control)
150
100
50
0
***
*
AIR
VAPE
AIR PT
C
HBEC
Apical glucose uptake
Glucose uptake (% control)
150
100
50
0
**
PBS
VAPE
PT